

Combining geostatistics and multiattribute transforms – A channel sand case study

Brian H. Russell, Daniel P. Hampson¹, Laurence R. Lines, and Todor I. Todorov¹

ABSTRACT

In this paper, we combine the methods of geostatistics and multiattribute prediction for the integration of seismic and well-log data, and illustrate this new procedure with a case study.

Our case study involves the prediction of porosity in the Blackfoot field of central Alberta. The objectives of the survey were to delineate the channel and distinguish between sand-fill and shale-fill. The input consisted of twelve porosity logs as well as a 3-D seismic volume, and the inversion of this volume. We found an excellent correlation between porosity and the inverted acoustic impedance volume. However, we found that the newly proposed method created an improved final result.

Our approach uses the well logs in the area to “train” the neural network. We first extract average porosity values at the zone of interest, and then compare these values to average seismic attributes over the same zone. The technique of cross-validation is then used to show which attributes are significant. We then apply the results of the training and cross-validation to data slices derived from both the seismic data cube and the inverted cube to produce an initial porosity map. Finally, we improve the fit between the well log values and the porosity map using cokriging. Our results are very encouraging, and delineate the channel sand much more clearly than on the original seismic volume, as well as giving a better fit to the observed well logs.

INTRODUCTION

The classical problem in seismic exploration and production is how to integrate seismic data, which is closely sampled spatially but of relatively low resolution, with well log data, which is of high resolution but is poorly sampled spatially. Traditionally, this has been done using a technique called inversion, which has been well described in the literature (e.g. Lindseth, 1979). There are numerous approaches to inversion, but most assume the convolutional model, extract an estimate of the earth’s reflectivity, and transform this reflectivity to impedance. Key problems that need to be overcome in inversion are the band-limited nature of seismic data, the presence of noise, and amplitude scaling issues. Thus, the final result is an approximation to the real goal, which is a spatially extended set of seismically derived well log curves that match the measured curves at the wells themselves. One way to improve the result is to add information from other seismic attributes, such as frequency, coherency, AVO intercept and gradient, and so on. Again, this requires a physical model that relates the seismic attributes to the well log data.

¹ Hampson-Russell Software Services Ltd, 510, 715 – 5th Avenue SW, Calgary, Alberta, T2P 2X6

An alternate approach for the integration of well log and seismic data is to use geostatistical methods such as cokriging and kriging with external drift (Doyen, 1988, Todorov et al, 1997). In this approach, the well log data is considered to be the primary dataset, and the seismic data provides a background trend. The advantage of this method is that the well ties are usually perfect, since these methods honour the primary variable exactly at the well tie itself. The disadvantage is that this perfect tie often implies a less-than-perfect physical model. For example, if cokriging is applied to the problem of tying seismic structure to picked well depths, the implied velocities often show “bulls-eyes” around the well intersections. More recently, multilinear regression and neural networks have been applied to predict well log properties from combinations of various seismic attributes (Hampson et al, 2001). In this approach, the well to seismic ties are considered to be the training points, and the statistical method being used “learns” the relationship between the attributes and the well values. The technique of cross-validation is used to prevent “over-training”. The results of the training are then applied to the complete seismic volume to create a reservoir parameter volume. The advantage of this approach is a good overall fit to the parameter of interest. The disadvantage is that the fit at the well ties locations is not exact.

In this paper, we combine the methods of geostatistics and multiattribute prediction, and show a geological application of this approach. In fact, we will actually combine all three techniques discussed in this introduction, since the key seismic attribute used in our case study turns out to be the seismic inversion attribute. Our example will involve a map-based approach, where the attributes are derived from an interval over the zone of interest of the channel sand.

CHANNEL SAND CASE STUDY

Before discussing the algorithms involved, we will briefly describe the case study to which these techniques will be applied. This study involves the prediction of porosity in the Blackfoot field of central Alberta. A 3C-3D seismic survey was recorded in October 1995, with the primary target being the Glauconitic member of the Mannville group. The reservoir occurs at a depth of around 1550m, where Glauconitic sand and shale fill valleys incised into the regional Mannville stratigraphy. The objectives of the survey were to delineate the channel and distinguish between sand-fill and shale-fill. The well log input consisted of twelve wells, each with sonic, density, and calculated porosity logs. The top and base of the sand zone for each of the wells was picked, and the porosity was averaged between the top and base as input to the mapping procedure. Figure 1 shows the distribution of wells throughout the 3-D survey area, as well as crossline 18 from the P-wave seismic dataset. Notice that the map has been rotated so that north to the right.

The seismic input consisted of two 3-D volumes. The first was the stacked P-wave seismic dataset from the survey, and the second was the acoustic impedance inversion of the initial seismic volume. This inversion was done using a model-based technique that can be described in two steps. First, an initial model is built from the well logs and seismic picks. Then, this model is perturbed until a best least-squares fit is obtained between the model-derived synthetic seismic and the original data. Figure 2 shows crossline 18 from the seismic survey, where (a) shows the input seismic line,

and (b) shows the inverted line. Notice that this line ties well 14-09, which is a dry hole, and 13-16, which is a producer.

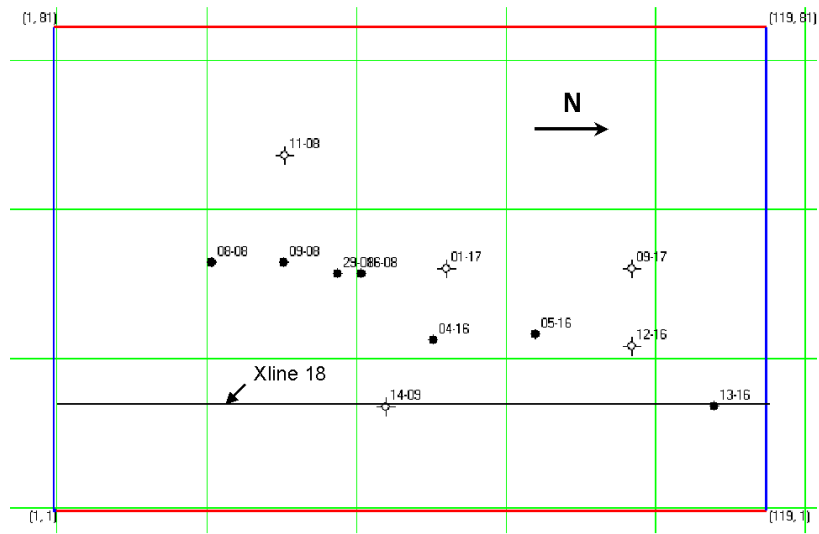


FIG. 1. The distribution wells within the 3D seismic survey area, Blackfoot oilfield, Alberta. The annotation shows inline and crossline numbers. Note that the map has been rotated so that north is to the right.

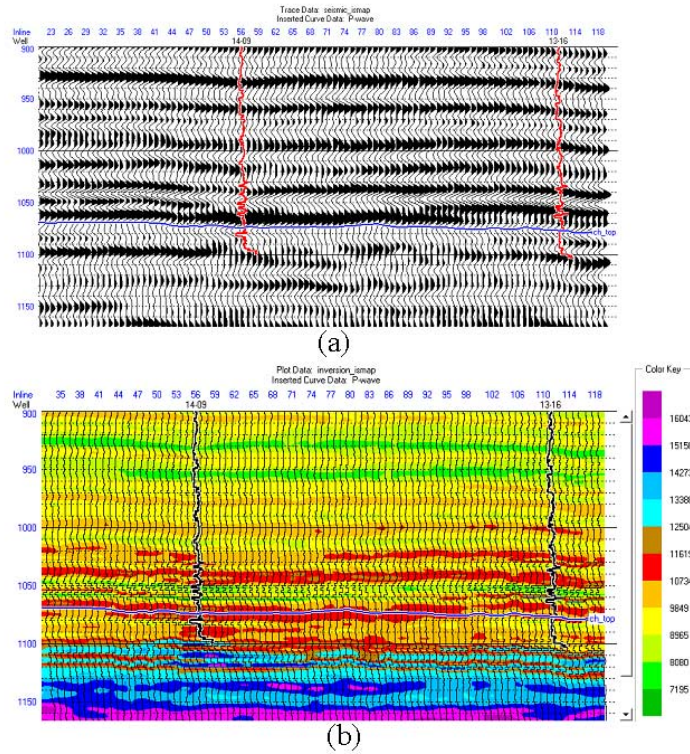


FIG. 2. Crossline 18 from the 3D seismic survey (see profile in Figure 1); (a) shows the final CDP stack, and (b) shows the impedance inversion.

Another key to this method is the extraction of a stable seismic wavelet to be used in the inversion process. Figure 3 shows the sonic and porosity logs for well 14-09, along with the seismic picks and log tops, and a portion of the seismic data at the tie point. The figure also shows the synthetic tie at the well intersection.

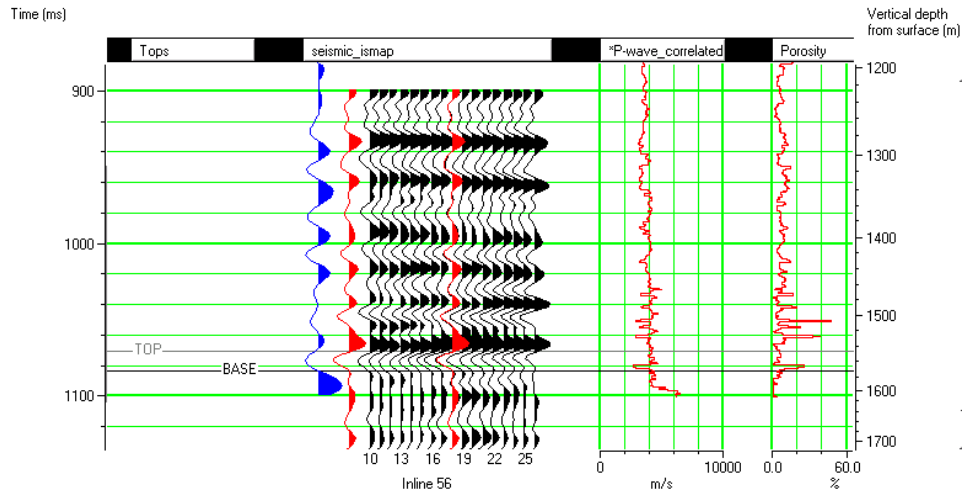


FIG. 3. Sonic and porosity logs from well 14-09, together with synthetic tie, seismic picks, and well log tops.

The porosity value at each well was then averaged between the top and base of sand. The resulting values have been plotted and colour-coded on the map shown in Figure 4. Notice the high porosity values in the centre left of the map.

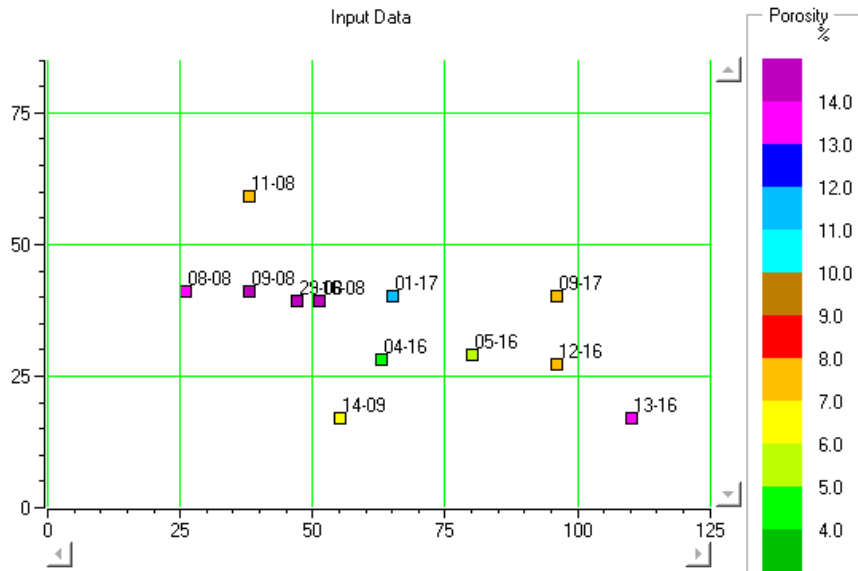


FIG. 4. The porosity of the sand interval at each well location, average between the top and base of the channel.

We next created a data-slice through the inverted impedance volume to use as the secondary dataset. To create this slice, the channel top was picked (this pick is shown on a piece of the seismic data in Figure 3), and then an arithmetic average from a 10ms window below the channel top was used to produce the slice. The resulting map

slice is shown in Figure 5. Notice the low impedance values on the middle left side of this map, indicating the possible channel.

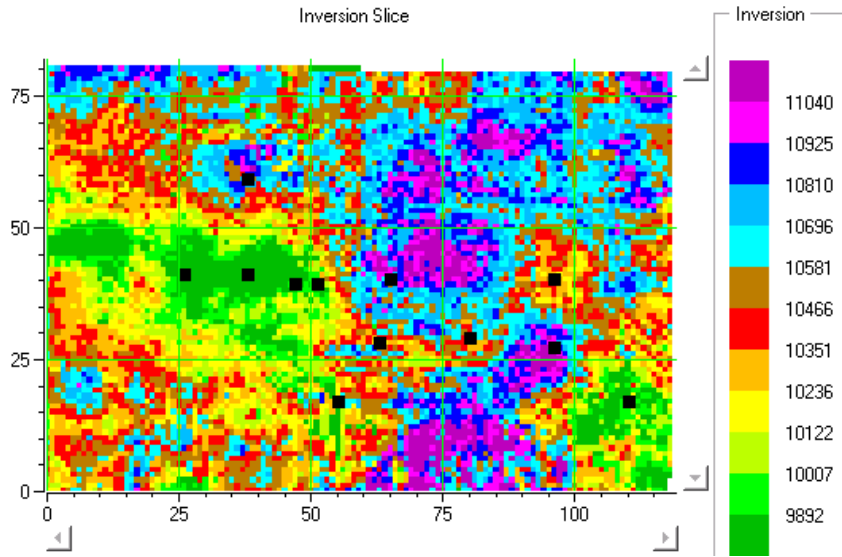


FIG. 5. Map of average acoustic impedance over a 10ms window below the picked channel top.

At the well locations, the average impedance values were then extracted from the map and crossplotted against the well porosity values. This crossplot is shown in Figure 6. Note that the correlation coefficient from the crossplot is equal to -0.65 . The negative correlation was due to the fact that porosity varies as the inverse of impedance.

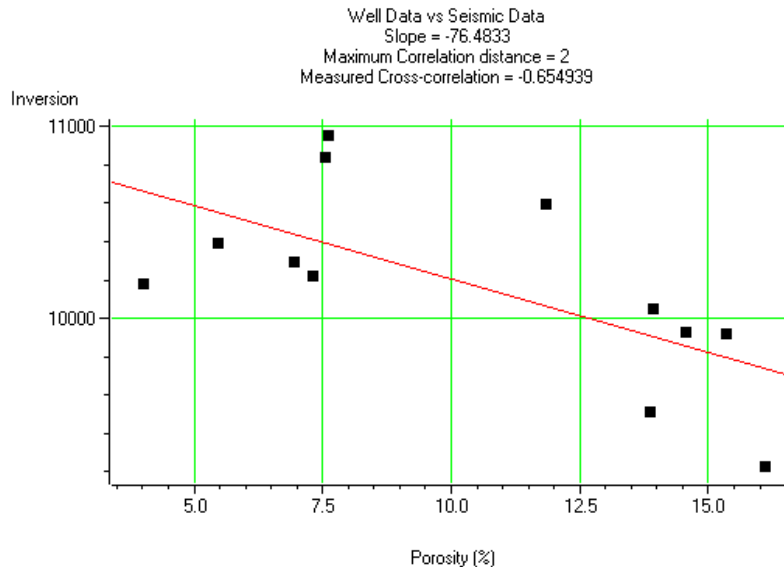


FIG. 6. Plot of average well porosity against average impedance for all the wells in the survey area.

The regression fit from this crossplot was then applied to the impedance slice to convert it to pseudo-porosity for display purposes. The resulting porosity slice is shown in Figure. 7. On this map, it is obvious that the well values do not tie the seismic values at the well locations, since the colour is indicative of porosity both at the wells and on the seismically derived map.

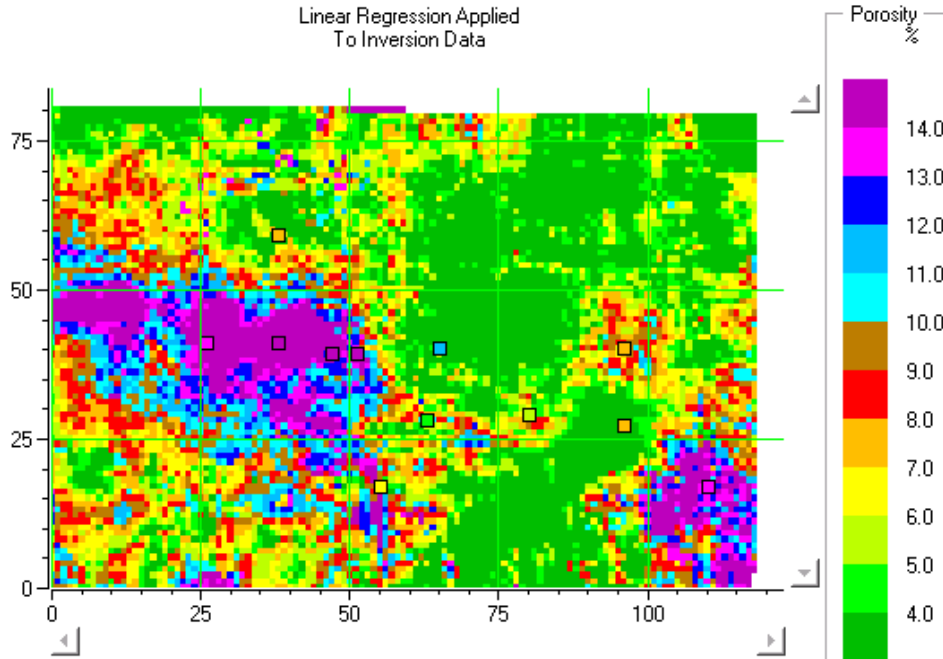


FIG. 7. Map of porosity variations in the survey area. This was derived by the application of the regression fit from Figure 5 to the impedance slice of Figure. 4.

MAP-BASED GEOSTATISTICS

Map-based geostatistics involves the integration of two related datasets. The primary dataset is generally a set of sampled values from well logs distributed throughout the map area. These values represent some reservoir parameter of interest such as porosity or depth. The secondary dataset is derived from a separate set of measurements, generally seismic data, which is related in some way to the primary dataset. For example, seismic amplitude or inverted seismic amplitude would be expected to correlate with porosity, whereas seismic structure time should correlate with measured well depth. To test the amount of correlation between the two datasets, a crossplot can be made between them, and both the regression line and the correlation coefficient can be computed.

The next step is to derive variograms from the well data and seismic data alone, and also from the well-to-seismic comparison. A variogram measures the spatial variability of the particular value being measured. That is, how does this parameter change as a function of distance? If there is very little spatial variability, the variogram will be close to zero, and if there is a lot of variability, the variogram will be large. In practice, the variogram is small for small distances close to zero, climbs rapidly, and flattens off to a uniform value.

Figure 8 shows two variograms, where (a) shows the well-to-well variogram and (b) shows the seismic-to-seismic variogram. In all of the following maps, a scaled version of the seismic-to-seismic variogram is used in the computations. This is referred to as the Markov-Bages approach.

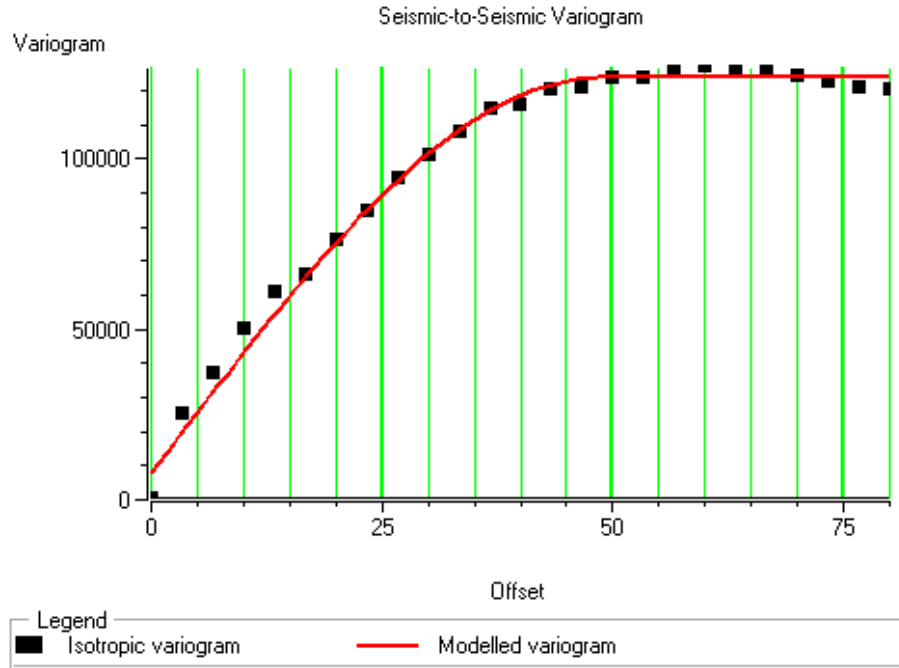


FIG. 8. The spatial variogram of (a) the well values and (b) the seismic values. The variogram is the sum of the squared differences between all the pairs of points within a given offset value.

The variogram is used to generate maps from the two datasets. If the well values alone are used, the technique for producing a best, linear, unbiased estimate of the unknown samples is called kriging. In the kriging process, each output sample is computed as a weighted sum of some, or all, of the input wells. That is, if the output porosity at a given map location is

$$\phi(x_0, y_0) = w_1\phi(x_1, y_1) + w_2\phi(x_2, y_2) + \dots + w_N\phi(x_N, y_N) \tag{1}$$

The weights in the kriging process are computed using the spatial covariance, which is derived from the variogram. Figure 9 shows the result of kriging the well values. Notice that the map shows only the general trends, which consist of high porosity on the left side of the map and low porosity to the right side of the map.

We also need an analytical way of judging the quality of our maps. Although many geostatisticians use the kriging error as their estimate, we feel that this estimate contains very little information content since it is highly dependent on the variance of the input values. A better measure of error, in our opinion, is the cross-validation error, which is found by successively leaving out wells and predicting their value. The cross-validation error for the kriged map is shown in Figure 10. The standard deviation of this error is 3.25%.

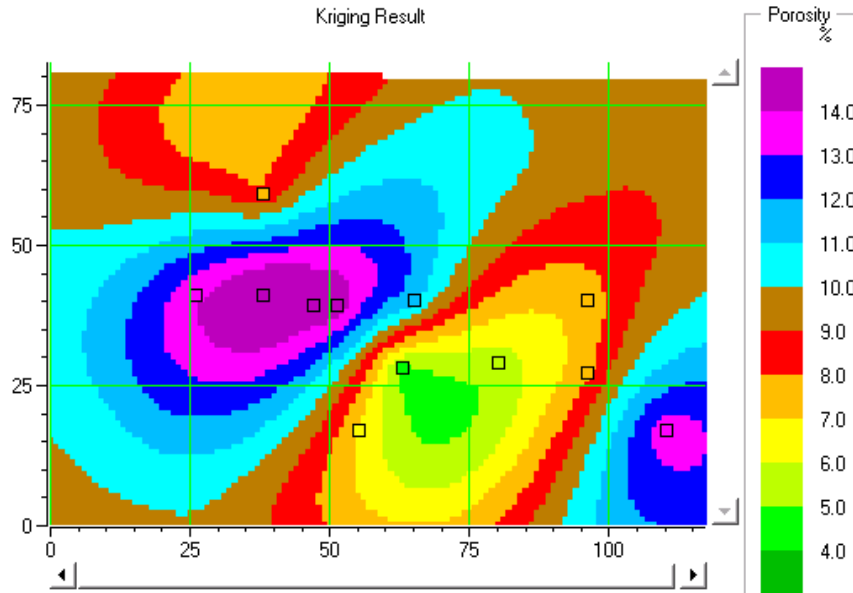


FIG. 9. Map of the survey area produced by kriging the well porosities (see text for details).

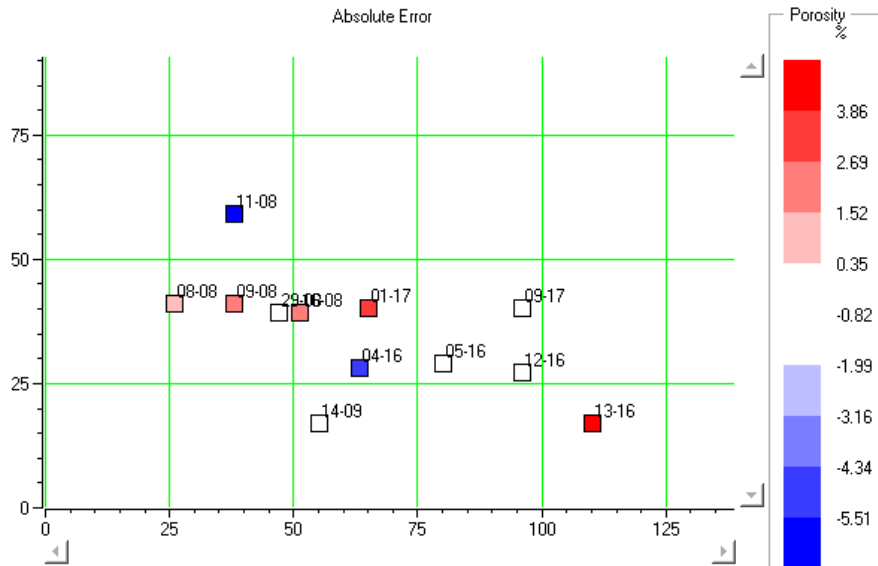


FIG. 10. The cross-validation error of the kriged map of Figure 9.

If we use both datasets, the techniques of kriging with external drift (KED) or cokriging can be used. For both these methods, the well-log data is considered the primary dataset, and the seismic is the secondary dataset. The quality of the final maps can be determined either through the cross-validation technique in which we leave each well out in turn and blindly predict its value, or a display of the error variance at each estimated point. In this paper, we chose to use the cokriging method rather than KED.

Cokriging is an extension of kriging that uses a weighted sum of both well and seismic values. In collocated cokriging, only the seismic value at the output location is used. The equation is therefore give as:

$$\phi(x_0, y_0) = w_1\phi(x_1, y_1) + w_2\phi(x_2, y_2) + \dots + w_N\phi(x_N, y_N) + w_{N+1}AI(x_0, y_0) \quad (2)$$

In the next result, Figure. 11, we combine the well and seismic data using collocated cokriging, which is a weighted sum of the well values and the seismic impedance value at the output location. This map also shows the imprint of the kriged result, or the wells. However, the standard deviation of its cross-validation is 2.91%, better than the kriging.

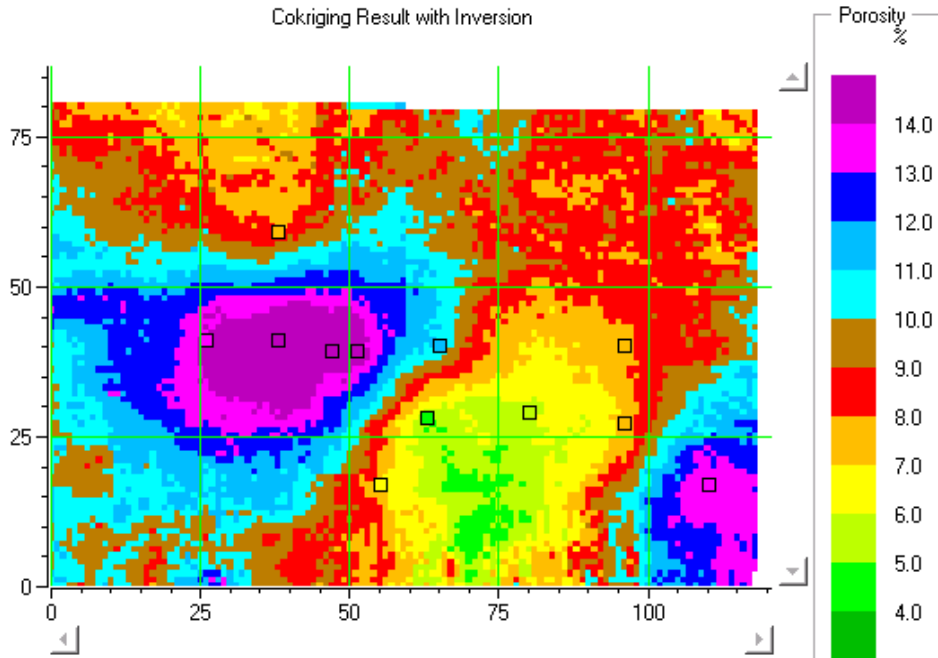


FIG. 11. Map of porosity in the survey area produced by collocated cokriging between the averaged well porosities and the impedance slice.

SEISMIC ATTRIBUTES

Before discussing the multiattribute method we will first discuss what we mean by the term, seismic attribute. The term seismic attribute has no universally accepted definition and can be interpreted as broadly or narrowly as is wished by an individual author. In this paper we choose a broad definition and define a seismic attribute as any dataset that has been derived from a poststack or prestack seismic volume, possibly constrained by a geological model.

To understand this more clearly, note that the seismic trace, $s(t)$, is usually modelled as the convolution of a seismic wavelet, $\omega(t)$, with the earth's reflectivity series $r(t)$ or:

$$s(t) = \omega(t) * r(t) \quad (3)$$

If the seismic trace is recorded at zero-offset, or zero angle-of-incidence, the reflectivity is related to changes in the acoustic impedance of the earth, where the acoustic impedance is defined as the product of P-wave velocity, times density. The

process of inversion, which was discussed in the previous section, attempts to recover the acoustic impedance of the subsurface. We consider inverted impedance to be a primary seismic attribute. The method that is used here to invert for acoustic impedance involves deriving a model from the well-log data for the low frequency component. The high frequency component is derived from the seismic data. A simple approximation to the inverted trace can be found by integrating the seismic trace.

Other attributes of interest are derived directly from the seismic data, and are often called instantaneous attributes (Taner et al, 1979). The two basic attributes are the amplitude envelope and instantaneous phase. The seismic trace, $s(t)$, can be thought of as the product of the amplitude envelope $A(t)$ and the cosine of the instantaneous phase $\cos\phi(t)$ shown below:

$$s(t) = A(t)\cos\phi(t) \tag{4}$$

Geologically, we can think of the amplitude envelope as responding to variations in acoustic impedance, and the instantaneous phase as measuring stratigraphic detail. A third common attribute is instantaneous frequency, $\omega(t)$, which is the time derivative of instantaneous phase, as shown below:

$$\omega(t) = \frac{d\phi(t)}{dt} \tag{5}$$

Instantaneous frequency measures the complexity of the reservoir, and is similar to another attribute, the trace length, which measures the total length of the seismic trace over a given window. To understand the concept of trace length, think of the seismic trace as a "snaked" string. The trace length is found by pulling the string tight and measuring its length.

For the multiattribute process, a series of slices was first extracted from the seismic cube. These slices were averaged over a 10msec window below the zone of interest, but using an RMS average, rather than an arithmetic average, since many of the attributes had zero mean (that is, both positive and negative values). The six slices that were extracted consisted of seismic amplitude, amplitude envelope, instantaneous phase, cosine instantaneous phase, trace length, and integrated trace. In the case of trace length, no averaging was performed since this attribute measures the length of the trace over the zone of interest. These slices are shown in Figure 12.

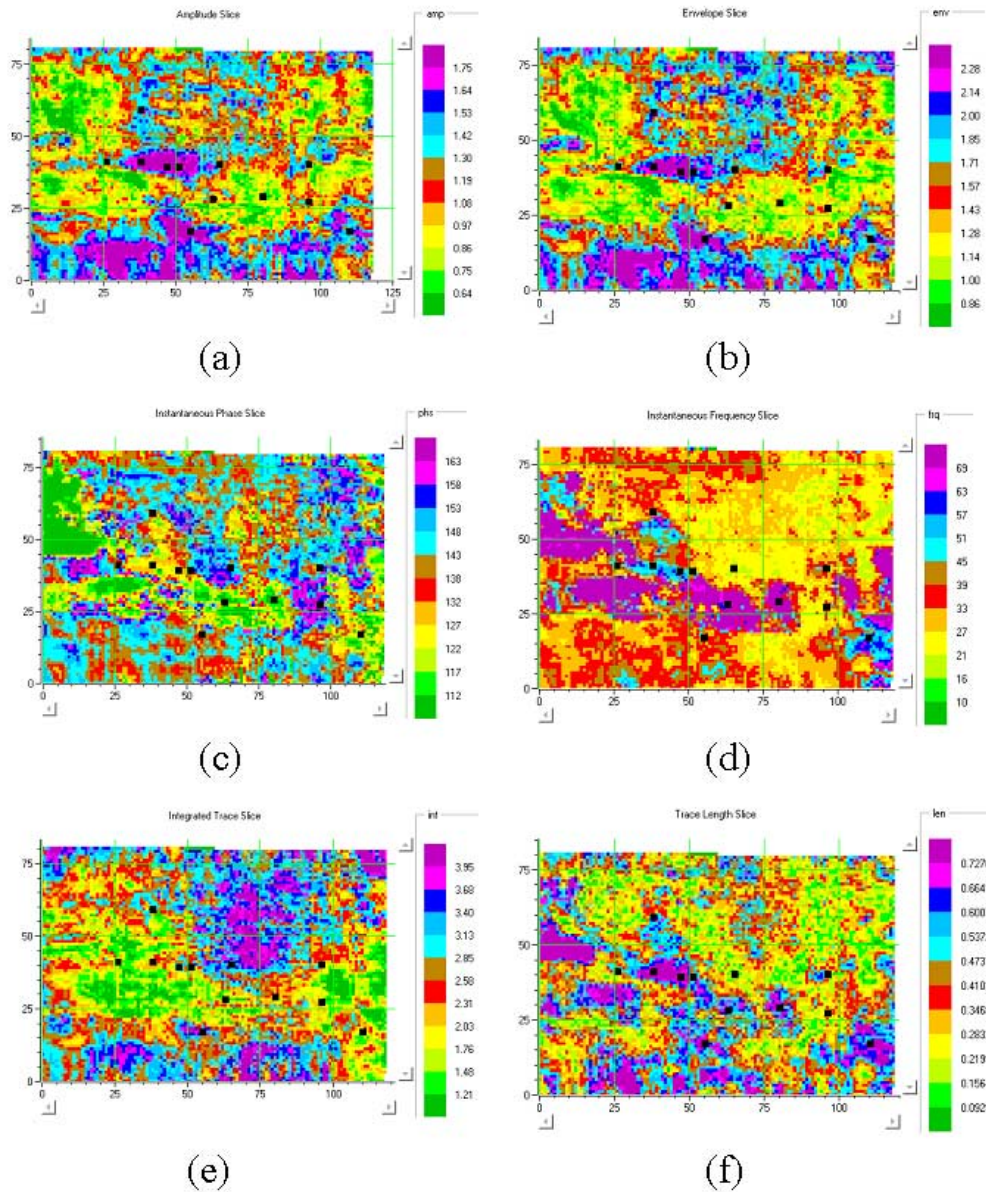


FIG. 12. Attribute slices derived from the original seismic volume, where (a) shows seismic amplitude, (b) shows amplitude envelope, (c) shows instantaneous phase, (d) shows instantaneous frequency, (e) shows integrated trace, and (f) shows total trace length. The first five attributes consist of an RMS average over a 10ms window below the picked channel top.

THE MULTIATTRIBUTE TRANSFORM

The multiattribute transform method involves the same input data as in the geostatistical method just described, except that multiple secondary sets of seismic measurements, or seismic attributes, are used. We will discuss what we mean seismic attributes in the next section. Another key difference between this method and the geostatistical method is that, in the multiattribute transform, an exact solution is not forced at the well-to-seismic intersections. Instead, a “best-fit” relationship is derived at the tie points, which is then applied to the multiple input attributes to produce the reservoir volume. Two approaches can be used to derive this relationship: multilinear regression and neural network analysis. In the multilinear regression approach, we seek a set of weights which, when applied to the attributes, will produce the reservoir volume. That is, we model the log parameter $L(x,y)$ as a weighted sum of the m attributes A_j by the linear equation

$$L(x, y) = w_0 + w_1 A_1(x, y) + \dots + w_m A_m(x, y) \quad (6)$$

In equation (1) both the estimated log values and the attributes are a function of the map coordinates x and y , rather than of time, t , as in the previous reference (Hampson et al, 2001).

Our second multiattribute approach involves combining the attributes in a nonlinear fashion. This can be done either by using nonlinear transforms on the attributes themselves (e.g. logarithm, square root, etc) or by applying neural network techniques. The neural network that we have found to be most effective is the probabilistic neural network, or PNN (Masters, 1995). Briefly, the PNN method is like a nonlinear extension to multilinear regression, where the weights are calculated using the concept of “distance” in attribute space from a known point to an unknown point. The weighting function is Gaussian with an inverse scaling parameter that can change for each of the input points.

For both the multilinear regression and PNN approaches, the number of attributes to be used is determined by the cross-validation method, in which the prediction error is computed by leaving out the target well for each of the input points, calculating the resulting least-squares error, and then summing the results. As we shall see shortly, the validation error will reach a minimum at a relatively small number of attributes, usually two or three.

First, let's see how well each of these slices correlates with the porosity values. This is shown in Table 1, where the first slice is the impedance slice, whose correlations coefficient we have already discussed. A multiattribute analysis was then performed at the well locations using multilinear regression. It was felt that there were not enough wells to justify using the PNN algorithm. The validation results for this analysis are shown in Figure 13. Note that the top curve is the validation result, in which the target well has been left out in the same way as described for our previous analysis.

Well Log Data	Seismic Data	Correlation
Porosity	Inversion	-0.654939
Porosity	amp	0.405974
Porosity	env	0.320297
Porosity	frq	-0.274947
Porosity	phs	0.153302
Porosity	len	0.110205
Porosity	int	0.0295412

Table 1. The correlation coefficients for the seven attribute slices.

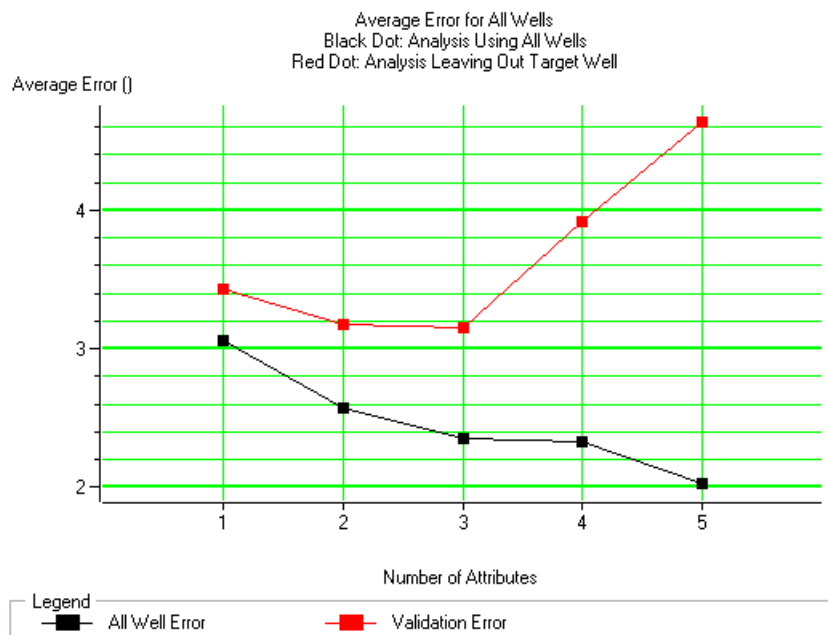


FIG. 13. The average error for the best five attributes found by multi-linear regression, where the bottom curve shows the total error, and the top curves shows the validation error.

Notice that only the first three attributes are statistically significant since the error on the top curve (which leaves out the target wells) increases after the third attribute. Table 2 shows a numerical summary of these attributes. Note that the three attributes were, in order, impedance, instantaneous phase, and integrated trace. Table 3 then shows the derived weights.

	Target	Final Attribute	Training Error	Validation Error
1	Sqrt(Porosity)	1 / (Inversion)	3.062634	3.428392
2	Sqrt(Porosity)	1 / (phs)	2.578627	3.173227
3	Sqrt(Porosity)	1 / (int)	2.353296	3.150217
4	Sqrt(Porosity)	(X-coordinate)**2	2.328632	3.731974
5	Sqrt(Porosity)	1 / (env)	2.286716	4.521664

Table 2. The three attribute slices used in the multiattribute computation.

Attribute Name	Attribute Transform	Weight
Inversion	1/X	110045
phs	1/X	-265.721
int	1/X	-1.24719
Constant		-5.05961

Table 3. The weights used in the multiattribute computation.

The results of applying the derived weights to the attribute slices are shown in Figure 14. Notice that the correlation coefficient has now increased to 0.82. Also, note the increased resolution of the high porosity sand channel in Figure 14.

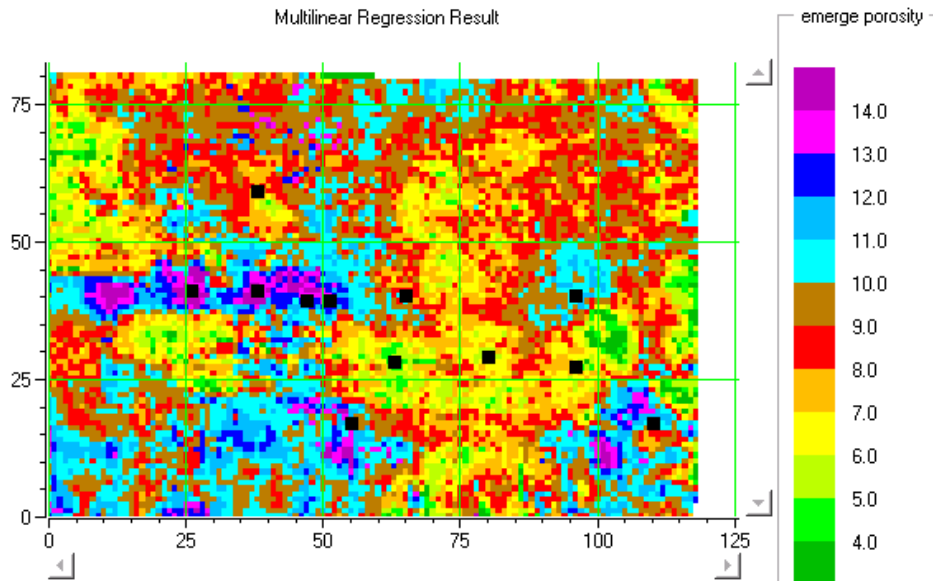


FIG. 14. The application of multi-linear regression to the impedance, instantaneous phase, and integrated trace attributes.

Although we have described the geostatistical method before the multiattribute method, the actual order of application is the reverse of this. That is, we first use the multiattribute method to produce an improved map as the secondary attribute for the geostatistical method. We then apply the technique of collocated cokriging to this new map.

As mentioned previously, we must first re-compute the variogram, and this is shown in Figure 15. In this case, we are using the Markov-Bayes linear assumption, and so we only need the seismic variogram to compute the cokriging result.

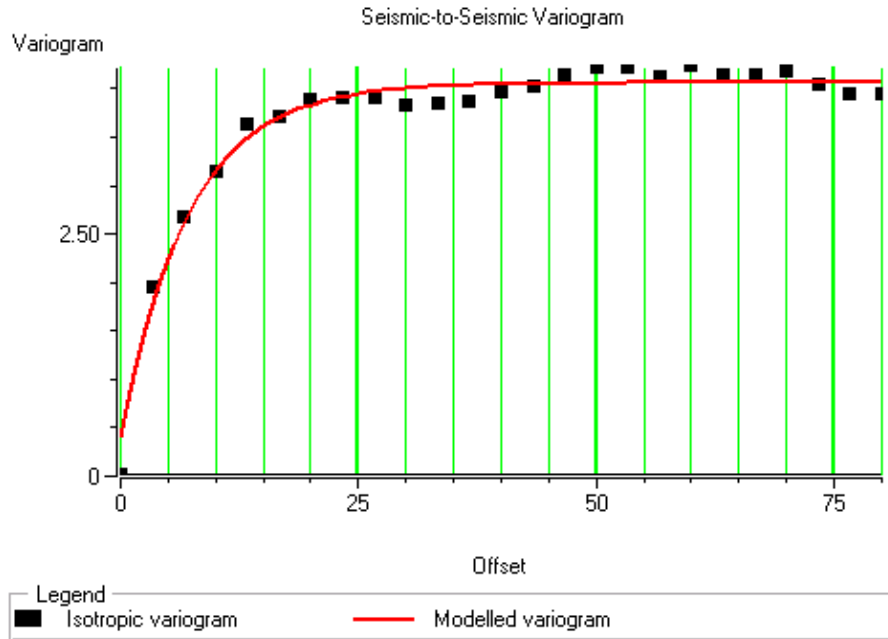


FIG. 15. The recomputed seismic variogram used for the final cokriging result.

The cokriged porosity result is shown in Figure 16. Notice that the channel sand is now clearly delineated, and the fit to the wells is very good. This is indicated by the color within the well symbols, which has the same range as the seismic values, and is indicated by the colour key on the right.

CONCLUSIONS

In this paper, we have presented a new approach to the integration of well log and seismic data, which combines the methods of seismic inversion, geostatistics and multiattribute transforms. Inversion is used as the starting point, since we have found that the inversion results correlate much better with geology than the original seismic. However, by using seismic attributes in addition to the inversion attribute in the multiattribute transform, we bring in extra information that can enhance the final tie. It is also important to use the technique of validation to make sure that we are not adding spurious attributes to the final solution. Finally, geostatistics gives us a powerful set of tools for producing our final map, which combines the multiattribute transformed map with the well values, giving priority to the well information.

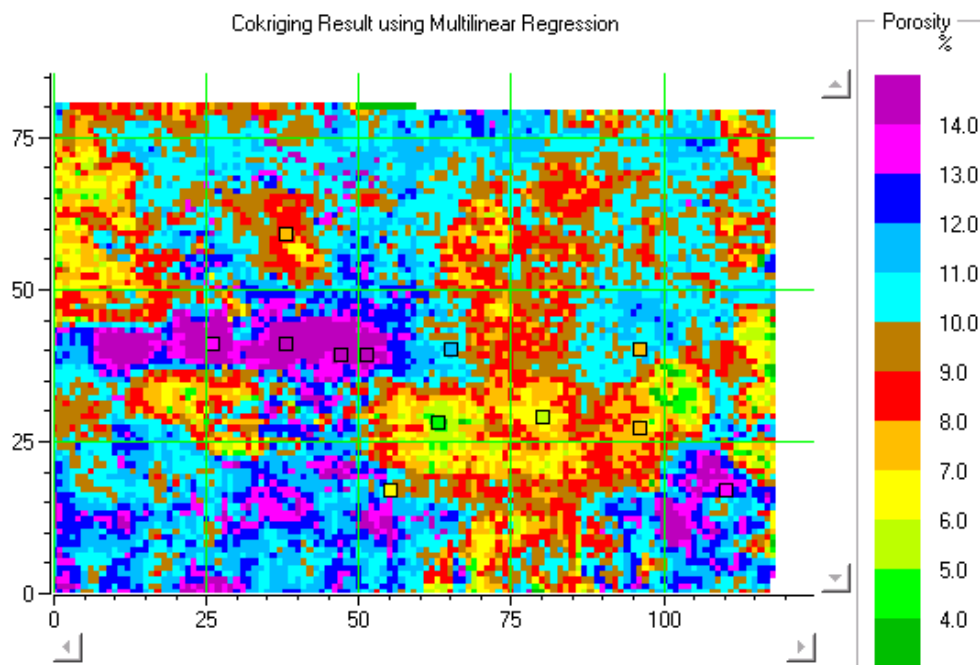


FIG. 16. The result of applying cokriging to using the multi-linear regression result.

Our method was tested using a channel-sand example from Alberta. We found that the correlation coefficient improved from 0.65 to 0.82 using the multiattribute method, and that the final KED result clearly delineated the channel sand, and provided an excellent match to the wells.

FUTURE WORK

Future work will involve research into alternate forms of neural networks that can be applied to this problem.

ACKNOWLEDGEMENTS

We wish to thank our colleagues at the CREWES Project and at Hampson-Russell Software for their support and ideas, as well as the sponsors of the CREWES Project.

REFERENCES

- Doyen, P.M., 1988, Porosity from seismic data – A geostatistical approach: *Geophysics*, 53, 1263-1275.
- Hampson, D., Schuelke, J.S., and Quirein, J.A., 2001, Use of multiattribute transforms to predict log properties from seismic data: *Geophysics*, 66, 220-231.
- Lindseth, R.O., 1979, Synthetic sonic logs-A process for stratigraphic interpretation: *Geophysics*, 44, 3-26.
- Masters, T., 1994, *Signal and image processing with neural networks*: John Wiley & Sons Inc.
- Taner, M.T., Koehler, F., and Sheriff, R.E., 1979, Complex seismic trace analysis: *Geophysics*, 44, 1041-1063.
- Todorov, T., Yang, G., and Stewart, R., 1997, Geostatistical analysis of 3C-3D seismic data for depth, isopachs, and sand/shale distribution: 1997 Technical Abstract Book, CSEG, 52.